ANALYSIS OF SURFACE TEMPERATURES IN URBAN AND SUBURBAN LANDSCAPES FROM SATELLITE THERMAL IMAGES: A CASE STUDY OF OLOMOUC AND ITS ENVIRONS, CZECH REPUBLIC

Jan GELETIČ, Miroslav VYSOUDIL

Abstract

The spatial variability of surface temperatures in the urban and suburban landscapes of Olomouc is analyzed in this paper, based on the evaluation of thermal satellite images from LANDSAT-5 (TM sensor) and TERRA (ASTER sensor). The temperatures of active surfaces were determined by the use of appropriate algorithms. Maps of surface temperatures are presented. The non-homogeneity of the active surface and thus also the relative difficulty of analysis of surface temperatures is documented by the land cover map. The surface field temperature was compared with the values of the air temperature recorded at the weather stations. The analysis showed that the description of spatial differences in surface temperatures of a city and its surroundings, based on an evaluation of the thermal imagery, was inconclusive. The differences reflect the seasons, but above all the nature of the land cover in the suburban landscape. These findings will be used in a study of the temperature regime of Olomouc and its environs.

Shrnutí

Analýza povrchové teploty v městské a příměstské krajině na základě analýzy satelitních termálních snímků, Olomouc a okolí (Česká republika)

Příspěvek se zabývá prostorovou variabilitou povrchové teploty v městské a příměstské krajině Olomouce na základě vyhodnocení řady termálních satelitních snímků LANDSAT-5 (senzor TM) a TERRA (senzor ASTER). Povrchová teplota byla stanovena použitím algoritmů vhodných pro uvedené senzory. Jsou prezentovány mapy povrchových teplot v městské a příměstské krajině v různých částech roku. Nehomogenitu aktivního povrchu a tím i poměrnou obtížnost analýzy povrchových teplot dokladuje mapa pokrytí země. Pole povrchové teploty bylo porovnáno s hodnotami teploty vzduchu zjištěnými na meteorologických stanicích Metropolitní staniční sítě Olomouc. Analýza ukázala, že popis prostorových rozdílů povrchové teploty středně velkého města a okolí z termálních satelitních snímků je nejednoznačný. Rozdíly odráží roční období, ale především charakter pokrytí země v příměstské krajině. Poznatky budou využity při studiu režimu teploty v městské a příměstské krajině Olomouce.

Key words: *satellite thermal image, land cover, active surface, land surface temperature, air temperature, urban and suburban landscape, MESSO (Metropolitan Station System Olomouc), Czech Republic*

1. Introduction

Differences between the climate of a city and the climate of its surroundings, i.e. between urban and suburban landscapes, can be studied in many ways. The most detailed approach can be considered to be a multilevel monitoring of the regime of selected meteorological elements. Air temperature plays an essential role among them. One of these levels, the highest one, is monitoring of the surface temperature survey of selected (most spread) active surface types obtained from satellite thermal images. The knowledge is important because the thermal regime of the ground layer of the atmosphere is among other things closely bound with the regime of surface temperature (Land Surface Temperatures, LST).

A major problem when dealing with focused research on this topic is the high degree of non-homogeneity of the active surface in the city and its surroundings, which results in a spatially highly variable and a complex array of surface temperature. This temperature is directly responsible for the temperature regime in the

ground layer of the atmosphere. This implies that an as accurate as possible knowledge of the land cover of the studied area is needed. The solution is the use of the database CORINE Land Cover, or determination of the surface type based on its emissivity or calculation from visible parts of the spectrum.

To verify the representativeness of results from the analysis of thermal images, we used - with respect to the functionality of the Metropolitan Station System Olomouc (hereinafter MESSO) – air temperature values recorded at the time of satellite passage, i.e., at moments when the photographs were taken. Air temperature in 2009 and 2010 was measured at 1.5 m above the active surface. For the year 2010, air temperature records were available from a limited number of stations measured at a height of 0.5 m above the active surface. Time differences of meteorological data readings and satellite scenes recording were insignificant. Maximum differences were 5' (LANDSAT-5) and 8' (TERRA).

Thermal satellite images have been used for some time in studying landscape and its components, especially in the field of climatologic research, and are described by many authors such as Adams and Gillespie (2006).

Van (2007) used remote sensing images from the ETM + sensor to determine relations between the type of land use and the surface temperature in an example of Ho Chi Minh city and its surrounding areas. LANDSAT satellite images were also analyzed by Nichol (1998) as described by Mesev (1998), who detected heat islands of Singapore and the Nigerian city of Kano. Calculating the surface temperature, he took into account the impact of buildings (geometry, height, number), which contribute to the resulting temperature value in densely populated areas.

The city heat island was studied also by Ozawa et al. (2004), who focused on densely urbanized areas in Japan. Nichol (1998) described average temperatures of individual agglomerations based on the evaluation of satellite thermal images. Detection of heat islands using thermal images in Brno was recently studied in details by Jelínek (2008) and Dobrovolný (2011).

Work on thermal imaging and obtaining information on surface temperatures was published by Weng and Yang (2006). They evaluated the Earth's surface temperature from a LANDSAT-7 image for studying factors contributing to air pollution in southern China. In other works, Weng, Lu and Schubringem (2004) and Weng and Lu (2006) studied the temperature field in Indianapolis using images from the satellites LANDSAT-7 and Terra (ASTER). Algorithms for obtaining surface temperatures were the same; they worked with surface categories to determine the emissivity values. Ganase and Lagiose (2003) used the night thermal imagery from LANDSAT-7 to obtain the surface temperature of the volcano Nissyros. The main objective was to assess the suitability of the LANDSAT image as a tool for monitoring the temperature regime of a volcano, using simple means of image processing (ERDAS, PCI). Stueven (2004) used thermal images of the Kilauea volcano from the LANDSAT satellite to compare temperature conditions on the images at intervals of three months. By unsupervised classification, using the ISODATA method, he obtained temperature scales which served only to compare temperature changes within the time interval.

2. Data and methods

During the implementation of this project, three data categories were analyzed – satellite thermal data, CORINE Land Cover database and meteorological data.

Satellite data

The selection of applicable satellite thermal images for the chosen period 2009–2010 was limited. One of the limiting factors was the existence of meteorological data from the Metropolitan Station System Olomouc (MESSO). The data were available in the desired range only for the years 2009 and 2010. The intention was to compare air temperature values measured at the stations with surface temperature values established by using thermal images. The second factor was that meteorological conditions characterizing the prevailing radiation weather had to exist in the studied locality at the time of taking the scenes by the satellite. Thus, only four scenes were available for the years 2009 and 2010 of the accessible databases of satellite images, moreover from different sensors. The used images then varied also by the spatial resolution in the thermal part of the spectrum.

Scene from 28th Sept. 2009, (9:52 UTC, 10:52 CET) was taken by the satellite TERRA and ASTER sensor and for the calculation of surface temperature it offers 5 thermal spectral bands (Band 10 – 8.125 to 8.475 μm, Band 11 – 8.475 to 8.825 μm, Band 12 – 8.925 to 9.275 μm, Band 13 – 10.25 to 10.95 μm, Band 14 – 10.95 to 11.65 μm) with a spatial resolution of 90 m.

Scenes from the satellite LANDSAT-5, sensor TM from 27th Sept. 2009 (9:34:43 UTC, 10:34:43 CET), 12th July 2010 (9:35:19 UTC, 10:35:19 CET) and 22th August 2010 (9:29:20 UTC, 10:29:20 CET) were in one thermal range 10.4–12.5 μm with a spatial resolution of 120 m.

Land cover data

Data on the character of the active surface were obtained from the CORINE Land Cover database 2006. Because the analyzed thermal images originated from different years and seasons, the information on the type of active surfaces were only preliminary. Describing the temperature field it was necessary to take into account the vegetation character in relation to the vegetation phase. Regarding the chlorophyll content and vegetation density, the values of surface temperature fields vary considerably during the stage of germination, ripening or at harvest time. The same applies, for example, for deciduous or mixed forests.

Meteorological data

Values of air temperature on days of taking the satellite images were obtained from measurements recorded at stations in the Metropolitan Station System in Olomouc (MESSO). The data were used to characterize the daily temperature regime during days on which the satellite scenes were scanned. At the same time, accurate values of air temperature were available at selected stations recorded at a height of 1.5 m at the time when the scenes were taken. Thus, it was possible to compare the surface temperatures and the corresponding air temperatures.

The ASTER scene was taken on 28th Sept. 2009, when the weather in the Czech Republic was under the influence of Wa situation. The oldest LANDSAT scene originates from 27th Sept. 2009, when the weather in the Czech Republic was also under the influence of Wa situation. The second LANDSAT scene is from 12th July 2010, when the weather in the Czech Republic was under the influence of Sa situation. Radiation weather (SWa situation) characterized the day of 22th Aug. 2010, when the last analyzed LANDSAT scene was taken. The daily course of temperature in those days was documented by records from the MESSO LETO station (Olomouc airport). The station in the outskirts of the town represents a typical suburban landscape. Active surface in its vicinity is formed by a well-kept lawn. Also, the daily temperature variation curves (Fig. 2) indicate the radiation regime of the weather.

2.1 Determination of surface temperature

Algorithms for determining surface temperatures

A common way for detecting actual surface temperature from the DN pixel value is known courtesy of physical laws. In specific cases, however, the calculation of surface temperatures is far more complex. The reason may be

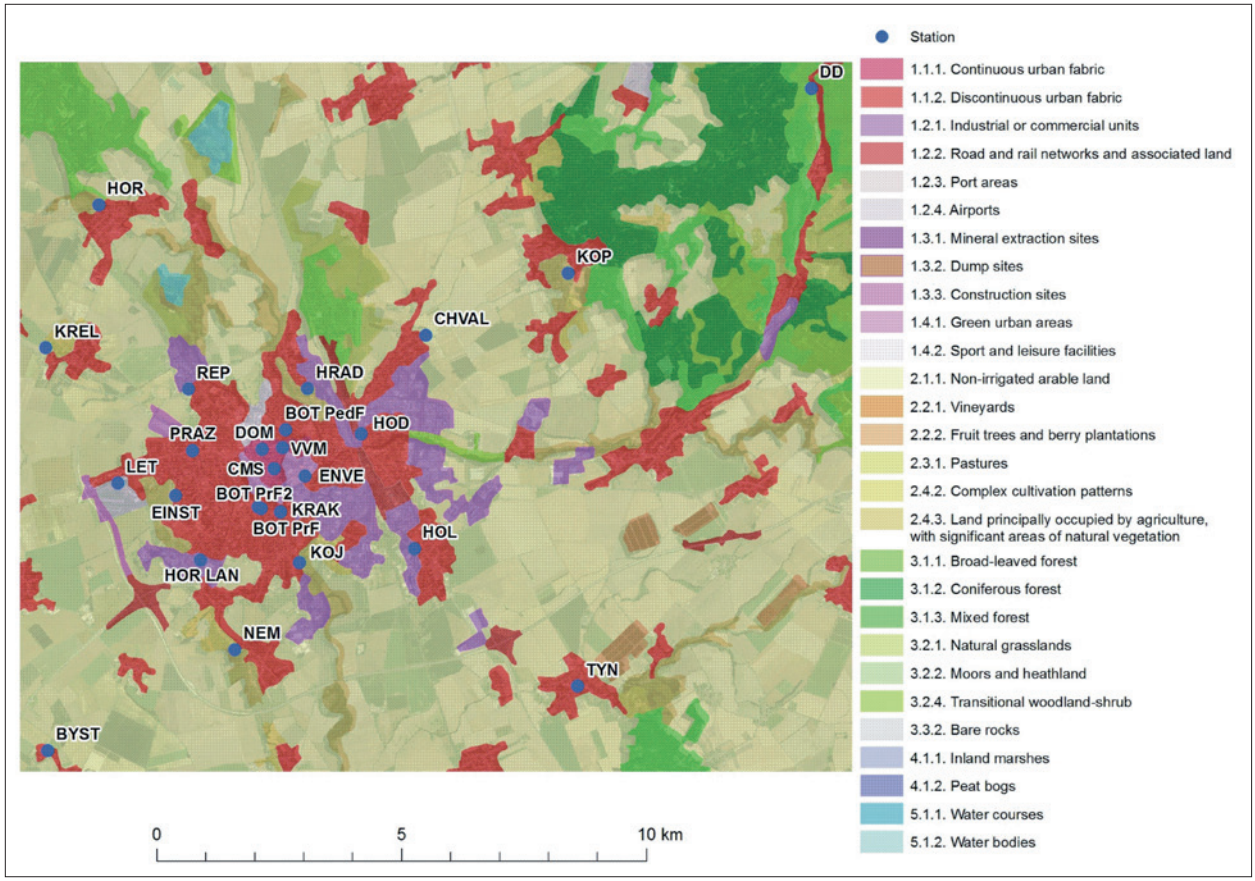

Fig. 1: Land Cover of Olomouc and surroundings with the MESSO network of stations (Source: CORINE Land Cover 2006, modified)

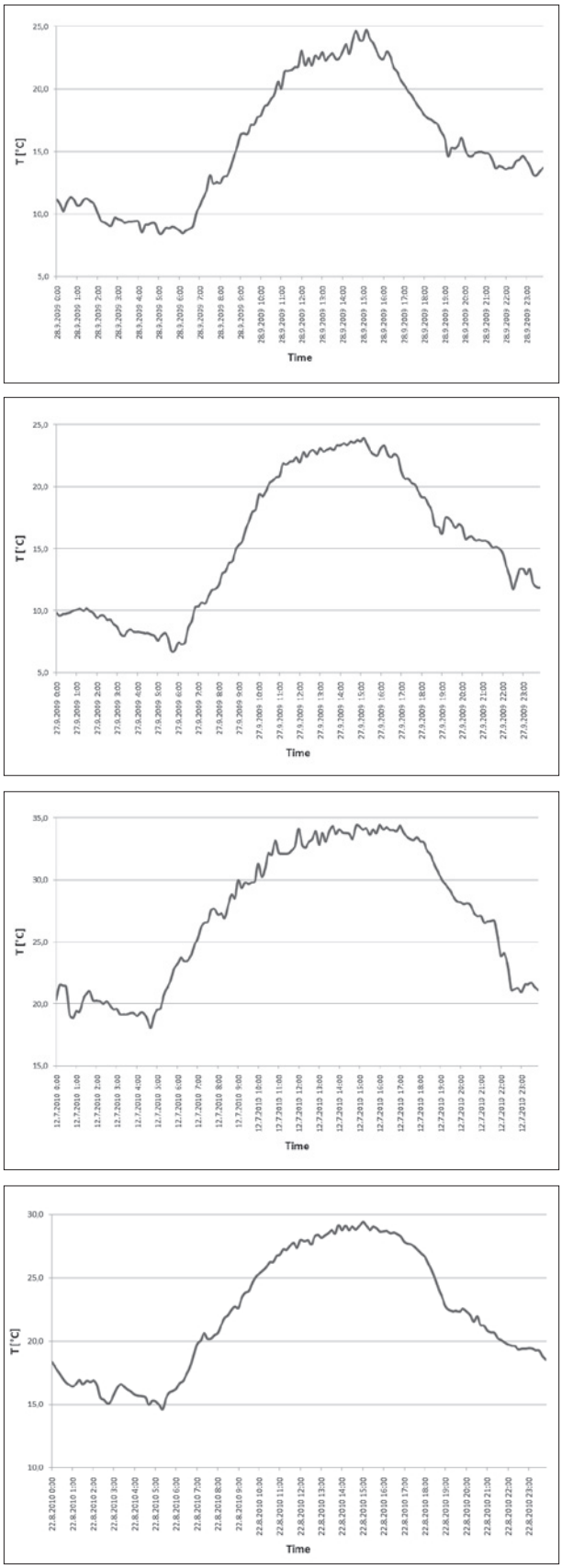

Fig. 2: The daily course of air temperature [°C] at the station MESSO LETO on days when thermal images were taken by the satellites ASTER a) 28th Sept. 2009 and LANDSAT b) 27th Sept. 2009 c) 12th July 2010, and d) 22nd Aug. 2010

both specifics of the digital photographic record of the image (number of thermal zones) and, for example, also a need to eliminate the effects of the atmosphere. A number of algorithms have been published by now that have often been developed for the calculation of surface temperature (LST, Land Surface Temperature) from a specific sensor. With this in mind, the algorithms in the text for the calculation of surface temperature are described with emphasis on a concrete application data from the LANDSAT-5 and ASTER sensors.

Liang (2004) divided the most frequently used algorithms for calculating the surface temperature into so-called split-window algorithms and multispectral algorithms. As to the number of thermal zones used in the first mentioned case, the algorithms in question use two or more thermal zones. Data from LANDSAT-5 encompass only one thermal zone and this is why we used the so-called mono-window algorithms. For the purpose of our paper, we used the mono-window algorithms and the split-window algorithms.

Mono-window algorithm for LANDSAT 5

Application of this algorithm is typical for LANDSAT satellites with only one thermal zone (in the case of LANDSAT-5 TM6). This relatively simple algorithm for detecting temperature, introduced by NASA (Quinn and Karnieli, 2001), has been used in many works dealing with the mapping of urban heat islands.

However, the algorithm using only one thermal band has the disadvantage in that the detected temperatures are not free from the influence of the atmosphere. Therefore, Quinn and Karnieli (2001) developed and applied an algorithm for data from LANDSAT TM6 that models the state of the atmosphere by means of two basic meteorological indicators of the state of the atmosphere – transmittance and average atmospheric temperature.

The algorithm can be divided into three phases, which are sub-steps in calculating surface temperatures from the original DN value. Firstly, it is necessary to convert the DN value to spectral energy density of radiation having the wavelength L_λ (i.e. range of wavelengths in which the band picks up the interval 10.4 to 12.5 μm falling upon the sensor in units $m^{-2}\,sr^{-1}\,\mu m^{-1}$):

$$L_{(\lambda)} = \frac{L_{min(\lambda)} + \left(L_{max(\lambda)} - L_{min(\lambda)}\right)Q_{DN}}{Q_{max}},$$

where $Qmax$ is the maximum possible DN value ($Qmax = 255$), Q_{DN} is DN pixel value, $L_{min(\lambda)}$ and $L_{max\,(\lambda)}$ are minimum and maximum detectable values of spectral density for $Q_{DN} = 0$ and $Q_{DN} = 255$.

According to NASA (2011), corresponding values for the LANDSAT-5 image are $L_{min(\lambda)} = 1.2378$ and $L_{max(\lambda)} = 15.303\ Wm^{-2}sr^{-1}\mu m^{-1}$, simplified as:

$$L_{(\lambda)} = 0.5515154\ Q_{DN} + 0.00485$$

Once the value of the spectral radiation is known, it is possible with the aid of the Planck function to calculate the radiation temperature T_{rad} [K] (brightness temperature), recorded by the sensor:

$$T_{rad} = \frac{K_2}{\ln\left(1 + \frac{K_1}{L_{(\lambda)}}\right)},$$

where K_1 and K_2 are calibration constants. Their values, according to NASA (2011) for LANDSAT-5 were determined as follows: $K_1 = 607.76\ Wm^{-2}sr^{-1}\mu m^{-1}$ and $K_2 = 1260.56$. If the emissivity of surfaces on the mapped area is known, a direct calculation of surface temperature is possible:

$$T_{KIN} = \frac{T_{RAD}}{1 + \left(\frac{\lambda T_{RAD}}{\alpha}\right) ln\varepsilon},$$

where λ is the wavelength of emitted radiation (in our case corresponding to the mean value of wavelength limits for LANDSAT thermal band) i.e.

$$\lambda = 11.45\ \mu\text{m},\ \alpha = hc / K = 1.4382 \times 10^{-2}\ \text{m}K$$

where K is the Stefan-Boltzmann constant, h is the Planck constant and c is the speed of light. The correction of temperatures to atmosphere is possible using the Karnieli and Quinn's formula (2001):

$$T_{KIN} = \frac{a(1 - C - D)(b(1 - C - D) + C + D)T_{RAD} - DT_A}{C},$$

where a, b are coefficients according to Quinn and Karnieli (2001) described in Tab. 1, T_A is average effective temperature of the atmosphere and for parameters C and D implies:

$$C = \varepsilon\tau, \qquad D = (1 - \tau)[1 + (1 - \varepsilon)\tau]$$

where ε is surface emissivity and τ is atmosphere transmittance.

It follows from the above that surface temperature corrected by atmospheric effect can be calculated from the radiation temperature. For this however, it is necessary to know the emissivity of surfaces and the average temperature and transmittance of the atmosphere. Surface emissivity can be calculated for example from NDVI index values (Liang, 2004), or the emissivity values can be established by using tables for the individual types of surfaces (Asmat, 2003).

According to Quinn and Karnieli (2001), the average temperature of the atmosphere can be derived – if more accurate data are not available - from air temperature at a height of 2 m by using the model of standard atmospheres. Transmittance can be calculated in a similar way from the values of water vapour content.

Multispectral algorithms

In the case of mono-window algorithm, the key knowledge for determining the surface temperature is that of emissivity, determined by some external means. This can be for example from vegetation indices, through the surface classification into several classes of known emissivity, or from other sources (e.g. CORINE Land Cover). By contrast, in the case of multispectral algorithms a very accurate way to determine emissivity is its detection directly from the thermal bands (Liang, 2004), i.e. by separating the information on surface temperature and emissivity directly from values recorded on the multispectral image. This is why the multispectral algorithms are referred to as "methods of temperature and emissivity separation – TES". The condition for the existence of multiple thermal zones and hence for the application of this method is met for instance by the sensors MODIS and ASTER.

For multispectral algorithms it is necessary to correct atmospheric effects before separating emissivity values and temperatures of a multiband thermal image. Then it is possible to determine both the surface temperature and the emissivity from the multi-spectral thermal image. However, effects of surface temperature and emissivity are so closely connected in thermal infrared radiation that their separation from thermal infrared radiation detected by the sensor is relatively difficult. This is because one multi-band thermal measurement of N zones represents N equations with N + 1 unknown factors (N emissivity values and surface temperatures).

Temperature range [°C]	Coefficients	
	a	b
0–30	– 60.3263	0.43436
10–40	– 63.1885	0.44411
20–50	– 67.9542	0.45987
30–60	– 71.9992	0.47271

Tab. 1: Coefficients of the calculation of atmospherically corrected surface temperatures according to Quinn and Karnieli (2001)

Without a priori information it is impossible to determine exactly either the surface temperature or emissivity. Most of these algorithms add to the system of equations one empirical equation in such a way that using the given N measurements (ranges) and this empirical equation is then possible to find out N + 1 unknown factors. Regarding the available data, key methods for this work are those dealing with data from the ASTER satellite (Gillespie et al., 1998; Gangopadhyay et al., 2005). The practical calculation of temperature is as follows. First, it is necessary to convert DN values into spectral density values for all thermal zones. According to NASA (2011 [online]), this is possible simply through multiplying the DN value by the value of the "band scale factor" coefficient (Tab. 2). The subsequent conversion of spectral density values to radiation temperature (T_{RAD}) was studied in detail by Alley and Jentoft-Nielsen (2001).

The influence of the atmosphere can be eliminated from thermal images by calculation, which uses only these thermal data (IEEE, 2004 [online]). The type of algorithms known under the name ISAC (In-Scene Atmospheric Compensation Algorithm) is often implemented in programmes designed for the processing of remote sensing images and is fully automated.

The algorithm assumes that atmosphere above the entire image is more or less homogeneous and that an object occurs on the scene whose radiation characteristics are very similar to radiation characteristics of a perfectly black body. However, it does not take into account the counter radiation of the atmosphere. First, the algorithm determines a wavelength, which most often radiates at a maximum radiation temperature. This wavelength is then considered as a reference. Only that part of the spectrum which has its radiation temperature on this wavelength is used to calculate atmospheric corrections. Dependences of absolute black body radiation and measured radiation values are then plotted for each wavelength in the correlation field. A regression line is fitted through this created field of points. Correction of this band is then applied as regression line slope and shift detected from the linear dependence of these data with the calculated absolute black body radiation at a corresponding wavelength.

Spectral band	Wavelength	Band scale factor
10	8.125–8.475	0.006882
11	8.475–8.825	0.00678
12	8.925–9.275	0.00659
13	10.25–10.95	0.005693
14	10.95–11.65	0.005225

Tab. 2: Parameter Band Scale Factor for the ASTER sensor

Upward radiation of the atmosphere and its transmittance can be expressed approximately as follows. First, surface temperature is determined for each pixel from the data and used to approximate radiation temperature using the Planck function and setting the emissivity value at a value of one. Then a regression line is fitted through the correlation field of the dependence of spectral density and radiation temperature. Upward radiation of the atmosphere and its transmittance are then obtained from the slope and the shift of the regression line.

Multispectral algorithms for ASTER

These algorithms known as TES were developed specifically for ASTER data. With their help, surface temperature and emissivity can be easily detected. They typically use a certain simplification for the reduction of unknowns (GILLESPIE et al., 1998). It should be noted that results of the practical application of these algorithms are often more focused on the use of emissivity rather than surface temperature, because exact emissivity is a very valuable source of information about the type of surface.

Normalized Emissivity Method (NEM)

This procedure calculates the surface temperature for each pixel and the range from data using a constant emissivity value. An often selected value for this constant is 0.95 or 0.96. The highest temperature is then regarded as temperature of the pixel. This high temperature serves also for the calculation of emissivity for the given pixel using the Planck function. These two methods were compared by Gangopadhyay et al. (2005) with data obtained from field measurements by using the precision radiation thermometer. A surface that was chosen for data validation was highly homogeneous water surface.

Calculation of surface temperatures

Of the two above-described methods, the mono-window algorithm for LANDSAT-5 is simpler. The procedure is relatively easy to implement in the GIS environment. The environment chosen for the work was that of ArcGIS 9.3. The biggest drawback of this algorithm is apparently the ignorance of emissivity of surfaces in the studied territory. Another disadvantage is a more difficult option of atmospheric corrections. Emissivity was calculated from the first three bands of the LANDSAT satellite by using the eCognition programme.

In the case of the algorithm for ASTER, it is not necessary to know the emissivity of surfaces. Even the atmospheric corrections are made by using the already pre-defined algorithms. Surface temperatures were calculated by using the ENVI 4.7 programme.

Surface temperature calculation for LANDSAT TM

Surface temperature was calculated by using the above-described mono-window algorithm applied in ArcGIS 9.3 (module ArcMap 9.3) using the extension of Spatial Analyst as a superstructure for working with raster data. Thus, surface temperatures are then corrected by the contribution of the atmosphere. The data flow is presented in a flowchart (Fig. 3).

The processing of the LANDSAT data consisted of two parts: map of radiation temperatures and map of surface emissivity. From these two parts, the surface temperature for each pixel can be calculated easily. Average effective atmosphere temperature can be detected by using the model of standard atmospheres. In this case, the following relation was chosen for the summer atmosphere of temperate latitudes (mid-latitude summer):

$$T_A = 16.0110 + 0.92621\, T_0$$

where T_0 is temperature at a height of two meters above the ground. At the time of the image taking the temperature was 20.36 °C. The value of transmittance was set at 0.8666750.

Surface temperature calculation for ASTER

Surface temperature was calculated by using the NEM algorithm because it is often applied in practice and is implemented in the software ENVI 4.7 used for the calculation. A characteristic difference of ASTER data processing is that the calculation of surface temperatures is entered by all five bands. First, it was first necessary to convert DN values to spectral density values and subsequently to correct them by the effect of the atmosphere. The actual surface temperature calculation by the NEM method requires entering the emissivity value on the input that will be used to calculate the temperature. The default value of 0.95 was chosen, which is -according to many available resources- the most frequently used value. The work procedure is shown in the diagram (Fig. 4).

2.2 Determination of the spatial differentiation of temperature field in urban and suburban landscape

In addition to the visual interpretation of the temperature field from the analyzed thermal images and land cover maps, the spatial differences on the selected pairs of images (ASTER 28th Sept. 2009 and LANDSAT TM 12th July 2010) were documented by parallel profiles of the surface temperature. Profile a) ran between the stations MESSO BYST-DDHL approximately in the SW-NE direction, profile b) between the stations HORK-VTYN in the NW-SE direction. The mentioned scenes showed the most significant surface temperature differences between the urban and the suburban landscape.

The values of surface temperature at the location of the selected stations were then compared with the values of the air temperature at a height of 1.5 m

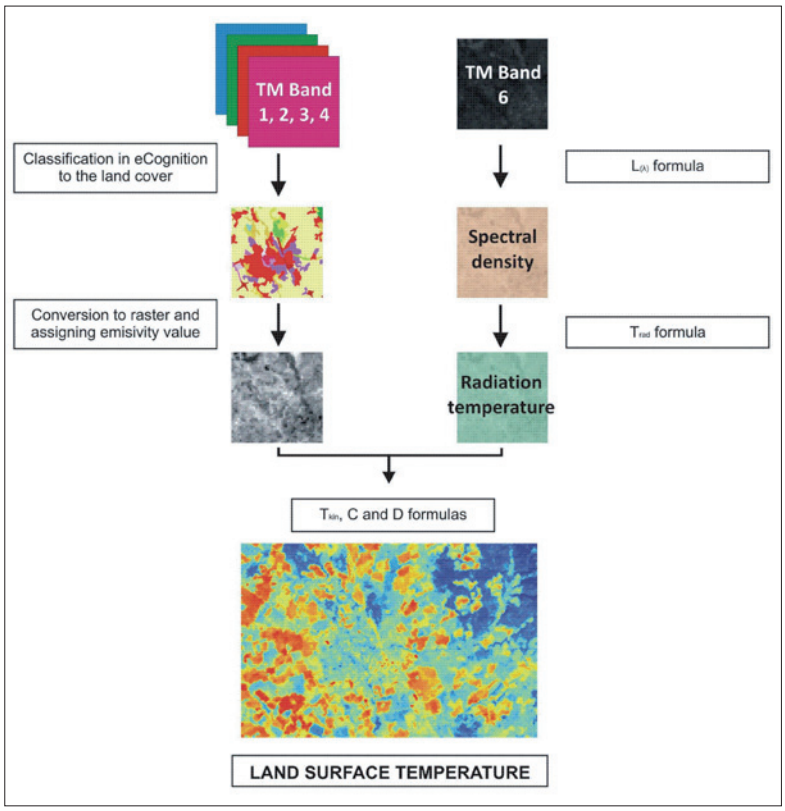

Fig. 3: Procedure of LANDSAT TM data interpretation

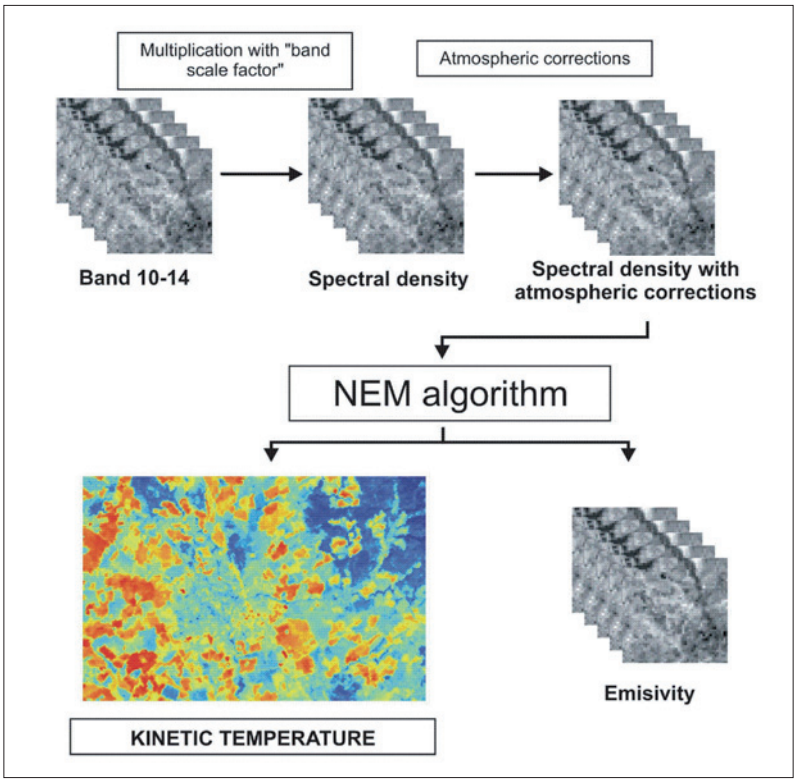

Fig. 4: Procedure of ASTER data interpretation

on these stations. Positive differences had been anticipated in favour of the surface temperatures. Empirical reasoning was sought for any negative differences based on the knowledge of the active surface character near the station. It was necessary to take into account the fact that the size of individual pixels was 90 × 90 m, resp. 120 × 120 m. On such an area, the active surface in the urban and suburban landscapes can be considerably inhomogeneous. As a result, there may be significant horizontal variations in the surface temperature (Figs. 6 and 9), which the thermal image cannot capture because of spatial resolution. However, if the station occurs within such a pixel and at the same time above the specific active surface, the temperature at this station may be affected exactly by its specific thermal properties. Then, its value may be lower than the corresponding calculated surface temperature of the given pixel.

3. Results

The presentation of results includes firstly the description of surface temperature field in Olomouc and its surroundings, as detected from the analysis of thermal LANDSAT and ASTER satellite images in four time periods in 2009 and 2010. All images were taken in the months of July, August and September, i.e. in the main growing season and at its end. It was especially this fact that affected the rate of temperature field differences between the urban and the suburban landscape. The second part of results is represented by air temperature values recorded on the MESSO meteorological stations at a height of 1.5 m above ground and their comparison with surface temperature values calculated for the station surroundings from the thermal images.

3.1 Surface temperature field

Generally it is assumed that the town's territory will show on thermal images with predominating artificial surfaces as significantly warmer. The results were not so conclusive, though, and the most likely reasons would be the time when the images were taken and the state of vegetation in the suburban landscape at that time.

The surface temperature field determined by analyzing the ASTER image from 28th Sept. 2009 (Fig. 5) is characterized by lower temperatures in the inner town. The warmest part of the town is represented by the SE part with a high concentration of artificial surfaces. Lower surface temperature values relate to most rural areas in the immediate surroundings of Olomouc. Significantly lower are the surface temperatures of forests and watercourses. Agricultural plots dominate in the suburban landscape as conspicuously warmer. The high temperature values of these plots reflect the thermal characteristics of bare cultivated farmland after harvest and agricultural work, i.e. in the absence of vegetation. The great horizontal variability of the temperature field in the autumn season is documented by temperature profiles between the stations BYST-DDHL and HORK-VTYN (Fig. 6).

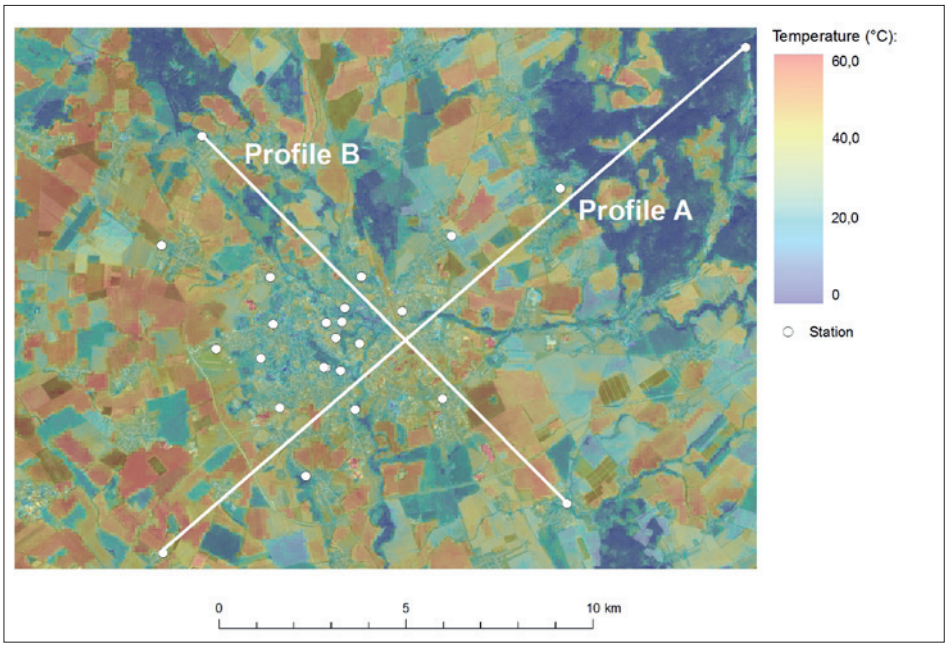

Fig. 5: Surface temperature field in Olomouc and surroundings on 28th Sept. 2009, 10:52 CET and the lines of surface temperature profiles a) BYST-DDHL, b) HORK-VTYN (source ASTER)

The LANDSAT image (27th Sept. 2009) was taken one day before the presented ASTER scene. The surface temperature field (Fig. 7 – see cover p. 2) is thus very similar to the analyzed ASTER scene. Neither the inner city nor the surrounding rural settlements show to be conspicuously warmer areas. They again represent agricultural areas with no vegetation in the suburban landscape. Forests in the NE part of the studied area are again clearly the coldest.

Very conclusive results about the function of urban areas as heat sources were harvested from analyzing the LANDSAT scene (12th July 2010). It was taken at a time when a greater part of agricultural areas surrounding Olomouc were covered by green vegetation whose thermal properties made it colder than the artificial surfaces of the city (Fig. 8 – see cover p. 2). As a heat island in the landscape, the town stands out quite clearly. This is also evident in the temperature profiles (Fig. 9) between stations a) BYST-DDHL and b) HORK-VTYN. Meteorological conditions undoubtedly played a role, since practically the entire second decade of July 2010 was characterized by tropical temperatures and the surface of the city was constantly overheated.

The surface temperature field in the urban and suburban landscapes of Olomouc obtained from the thermal image Landsat (22th Aug. 2010) shows insignificant spatial differences (Fig. 10). Artificial surfaces of the inner city and agricultural areas in the post-harvest season behaved almost identically. However, the warmer area in the city is once again represented by its SE and S parts. Extensive areas of "green" forest stands and larger water bodies are clearly the coldest.

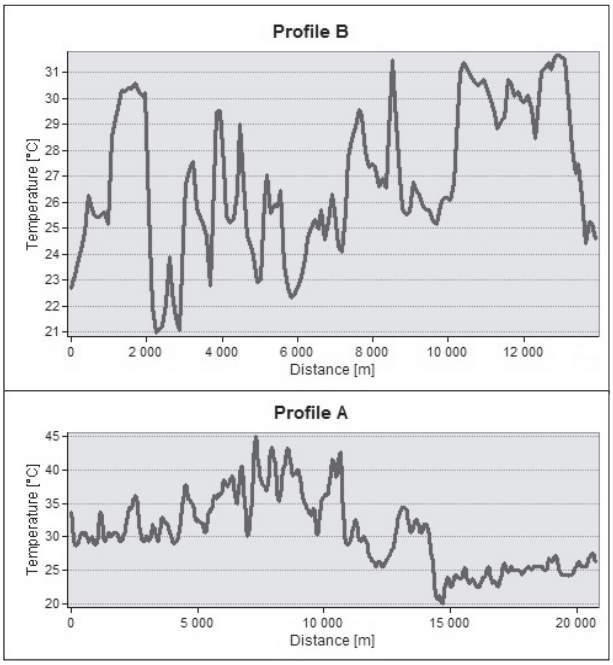

Fig. 6: Surface temperature profile between the stations a) BYST-DDHL, b) HORK-VTYN

3.2 Surface temperature and air temperature

The relevance of surface temperature values established by analyzing thermal satellite images was assessed by comparison with the air temperature values recorded by MESSO at a height of 1.5 m ((Tab. 3). Temperature records from the KOPE, DDHL, BOT_PeF, LETO, BYST and DOMI stations were available for all days, whereas from the stations ENVE, JUTA they were available only for 12th July 2010 and 22th Aug. 2010.

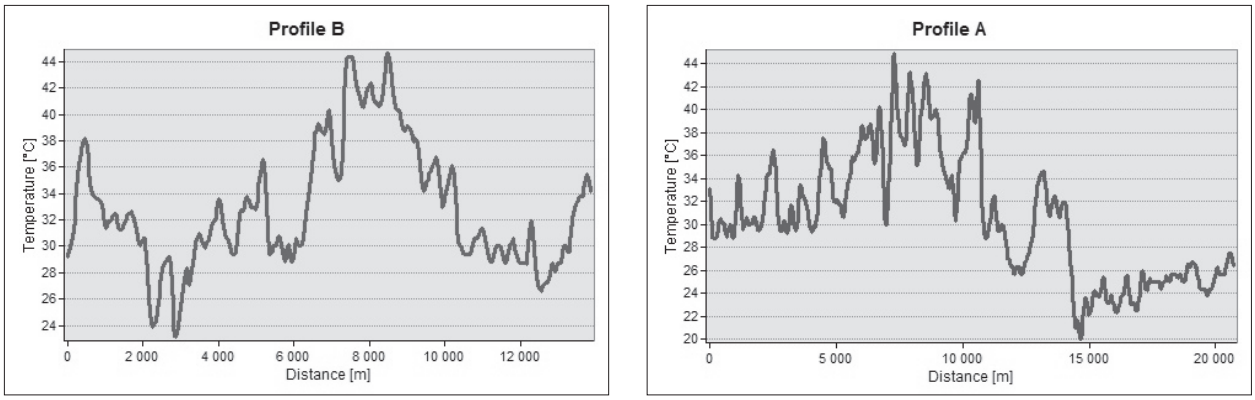

Fig. 9: Surface temperature profile between the stations a) BYST-DDHL, b) HORK-VTYN

Surface temperature (LST)

The level of surface temperature at selected stations in all time periods is evident from Fig. 11. It follows quite clearly from these data that the suroundings of the DOMI, JUTA and LETO stations are the warmest at all times. As the stations are of typically urban and suburban (LETO) character, it can be stated that the temperature is affected here mainly by the nature of the active surface.

On the other hand, always cooler were the DDHL, KOPE and BYST stations (except for the date 28th Sept. 2009). None one of these stations is typically urban. In these cases, we are probably dealing with a combination of the georelief form and active surface effects on the temperature regime.

A very similar character of the surface temperature field was observed on the ENVE and BOT_PeF stations. These represent the type of town stations with the ENVE station being located on the flat roof of a building and the BOT_PeF in the botanic garden. The types of the active surface are rather similar at these stations (gravel or land with sparse grass stand).

Regime atmosphere temperatures in the study area on 12th July 2010 document the air temperature values at 1.5 and 0.5 m above surface, where at most stations the values on the ground are significantly higher and reflect properties of the active surface in their vicinity (Tab. 4, Fig. 11).

The principle of warming the ground atmosphere on 22th Aug. 2010 from the active surface confirm the value at the stations MESSO at heights of 1.5 m above surface (Tab. 4).

Air temperature

The values of air temperature at 1.5 m above the ground for all days were available only for stations presented in Tab. 3.

From Tab. 3, it is obvious that air temperatures on the observed days and times characterized the temperature of individual stations generally in the same manner. While the DOMI and BOT_PeF stations were practically always the warmest, the DDHL, LETO and BYST stations ranked with the coldest ones.

Relation between surface temperature and air temperature

With respect to the warming of the ground atmosphere layer, surface temperature should be higher than air temperature, or the two should be equal. The obtained results confirm this assumption only partially (Tab. 4).

The analysis of scenes from the year 2009 confirmed the theoretical assumption of lower air temperatures with the exception of that recorded on 27th Sept. at the BYST and DDHL stations. The number of cases where the surface temperature values in the surroundings of the stations in 2010 were lower than those at 1.5 m above the ground was incomparably higher. The situation occurred on 12th July and 22th Aug. on the stations BOT_PeF, DDHL and KOPE.

When assessing the level of surface and air temperatures by individual stations, then the surface temperature was always higher at stations ENVE, DOMI, JUTA and LETO. Lower surface temperature occurred in three cases at the stations BYST and DDHL.

As to the date of taking the thermal scene, the situation was more difficult. The always higher surface temperatures recorded on the measuring days at the stations BOT, DOMI, KOPE and LETO reflect characteristics of the surroundings of these stations where the active surface can be considered as homogeneous or consistent with the active surface in larger surroundings.

It is worth mentioning that on 28 Sept. when a higher surface temperature in the vicinity of all stations was recorded, the object of the analysis was the ASTER thermal image with a higher spatial resolution (90 m).

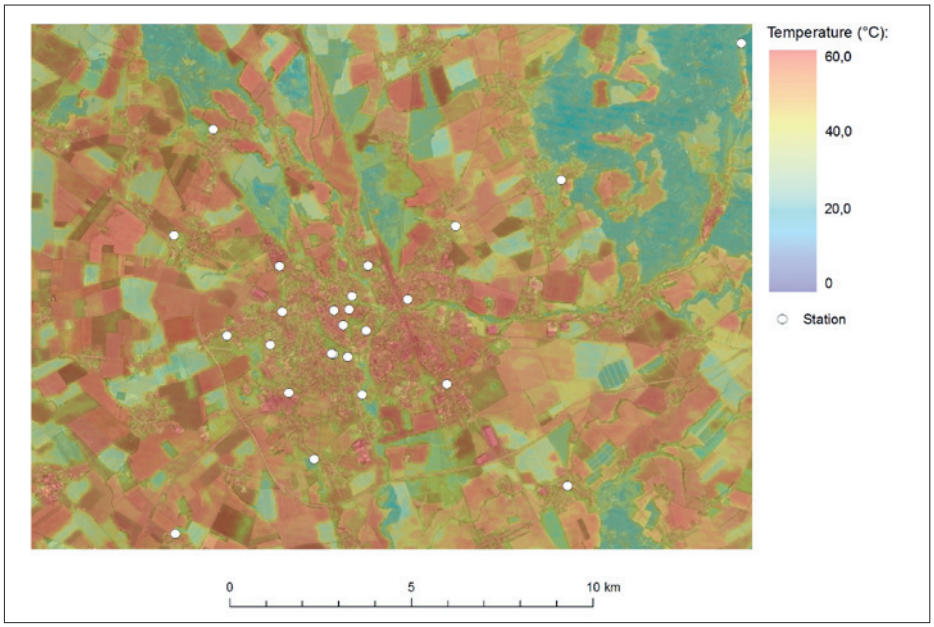

Fig. 10: Surface temperature field in Olomouc and its surroundings on 22th Aug. 2010 (source LANDSAT TM)

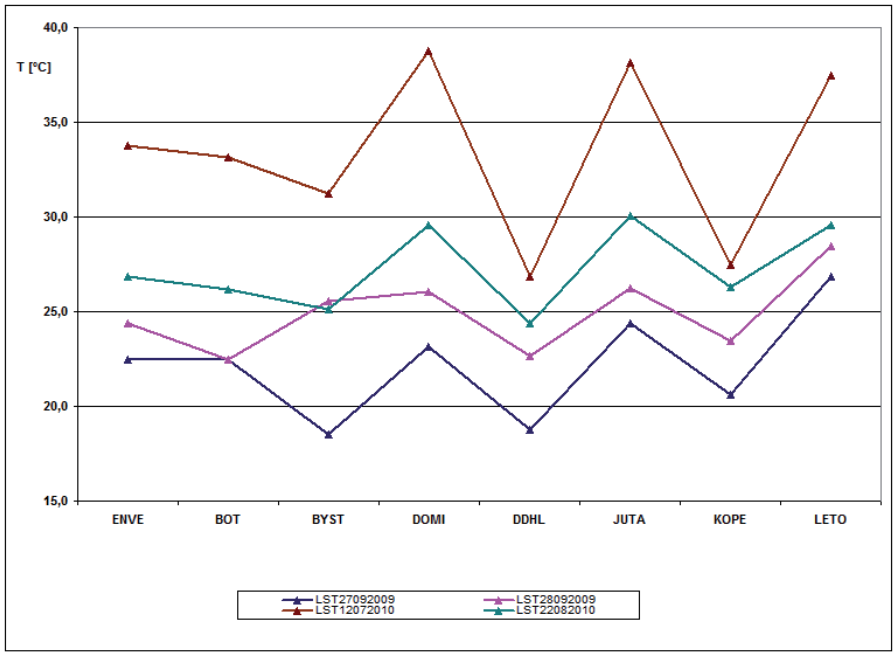

Fig. 11: Surface temperature (LST °C) in the suroundings of the selected MESSO stations, determined from ASTER satellite thermal images (LST22082010) and LANDSAT TM (LST27092009, and LST28092009 LST20072010)

Lower surface temperatures characterize at all times surroundings of the stations BOT-PeF, BYST, DDHL and KOPE. The reason may have to do with the location of the stations and namely with the character of the active surface. Both factors may be the reason why the surface was not sufficiently warmed up in the morning under the radiation weather and immediately above it a very thin inversion layer could have developed.

This is why the air at 1.5 m above the ground could have been warmer than the ground surface itself. A certain role could have been also played by the 120 m spatial resolution of the scenes, where the inhomogeneous active surface might have affected the calculation.

The rate of dependence between air temperatures on 12th July 2010 and 22th August 2010 recorded at all stations is expressed by the correlation coefficient 0.5407; the level of dependency between the values of surface temperatures on the same days was expressed as 0.9041.

The rate of correlation between the value of difference (LST-AT) and LST 22th Aug. 2010 is expressed by 0.9236; for 12th July 2010 it was 0.7104, which can be considered as values statistically significant.

Station	27th Sept. 2009	28th Sept. 2009	12th July 2010	22th Aug. 2010
BOT_PeF	20.8	22.0	33.8	27.3
BYST	20.9	20.2	32.8	26.4
DOMI	22.1	21.8	34.2	27.4
DDHL	21.0	20.2	31.6	26.0
KOPE	20.6	21.3	33.3	27.2
LETO	20.3	20.6	32.1	26.2

Tab. 3: Air temperature (AT °C) on 27th Sept. 2009, 28th Sept. 2009, 12th July 2010 and 22th Aug. 2010 on the selected MESSO stations at the time when the thermal images were taken

Station	Date	AT	LST	LST-AT
ENVE	27. Sept. 2009*	x	22.50	x
	28. Sept. 2009*	x	24.39	x
	12. July 2010*	33.49	33.75	0.26
	22. Aug.2010**	25.11	26.83	1.72
BOT_PeF	27. Sept. 2009*	20.78	22.50	1.72
	28. Sept. 2009**	22.00	22.47	0.47
	12. July 2010*	33.83	33.12	– 0.71
	22. Aug. 2010*	27.29	26.17	– 1.12
BYST	27. Sept. 2009*	20.90	18.50	– 2.40
	28. Sept. 2009**	20.20	25.54	5.34
	12. July 2010*	32.80	31.25	– 1.55
	22. Aug. 2010*	26.36	25.12	– 1.24
DOMI	27. Sept. 2009*	22.12	23.12	1.00
	28. Sept. 2009**	21.79	26.07	4.28
	12. Kuůy .2010*	34.22	38.75	4.53
	22. Aug. 2010*	27.39	29.56	2.17
DDHL	27. Sept. 2009*	21.01	18.75	– 2.26
	28. Sept. 2009**	20.18	22.67	2.49
	12. July 2010*	31.57	26.87	– 4.70
	22. aug. 2010*	25.95	24.40	– 1.55
JUTA	27. Sept. 2009*	x	24.37	x
	28. Sept. 2009**	x	26.24	x
	12. July 2010*	33.80	38.12	4.32
	22. Aug. 2010*	27.40	30.04	2.64
KOPE	27. Sept. 2009*	20.58	20.63	0.05
	28. Sept. 2009**	21.30	23.43	2.13
	12. July 2010*	33.29	27.50	– 5.79
	22. Aug. 2010*	27.18	26.30	– 0.88
LETO	27. Sept. 2009*	20.28	26.86	6.58
	28. Sept. 2009**	20.56	28.47	7.91
	12. July 2010*	32.14	37.50	5.36
	22. Sept. 2010*	26.24	29.56	3,32

*Tab. 4: Air temperature (AT °C) at 1.5 m above ground surface on selected MESSO stations at the time of taking the images; surface temperature (LST °C) on thermal satellite images for the surroundings of these stations and their difference (LST-AT °C), (** ASTER, * LANDSAT TM, x - data were not available)*

4. Discussion and conclusion

The objectives of this research project concentrated on the analysis of the surface temperature field and its spatial differentiation in the urban and suburban landscapes of Olomouc from satellite thermal images. The available scenes made it possible to achieve this goal, even though the selection for the period 2009–2010 was very limited. A partial objective was to compare surface temperatures in the surroundings of selected MESSO stations with air temperatures at 1.5 m above the ground surface for these stations at the time when satellite scenes were taken. This part of the research, too, produced results which appeared to be complicated.

For the comparison of results from individual scenes, it is useful that the scenes were taken approximately at the same time. A less advantageous aspect is that the scenes were taken only in the months of July and August when the state of vegetation in its developmental stages very distinctly affects the possibility of the transformation of radiant solar energy to heat energy and the degree of its radiation into the ground layer of the atmosphere. This was probably one of the main reasons why the apparently most conclusive results were harvested from the scene taken on 12th July 2010.

Further interpretation of temperature field differences between the urban and suburban landscapes made use of air temperatures recorded by the MESSO stations at a height of 1.5 m above the active surface at the time when the satellite scenes were taken. This made it possible to assess causal local relations between surface and air temperatures. Not always and not at all stations the temperature stratification was unstable. Relatively often the surface exhibited temperatures lower than those of the adjacent ground-level atmosphere at 1.5 m above the ground. It turned out that active surface in the surroundings of the station plays a more important role than the type of the station (urban, suburban).

Based on the research results it can be stated that the applicability of commonly-available thermal satellite images for the description of temperature field differences between the urban and suburban landscapes of a medium-sized city is possible, with some limitations. The main limitation is the season of the year because the non-existence of green vegetation may give rise to heat islands (thermal spots) also in the suburban landscape (Fig. 7). In this sense, the effect of forest stands is very distinct as obvious from the analyzed scenes.

Another limitation is the spatial resolution of thermal satellite images. Evidence of this can be lower surface temperatures recorded in many cases on the LANDSAT scenes (120 m) as compared with air temperatures recorded on the meteorological stations. In case of the ASTER scene (90 m), surface temperatures in the surroundings of the MESSO stations were at all times higher than the corresponding air temperatures. The specification of warmer or colder areas from satellite thermal images appears only of informative character in the case of medium-sized cities. A more precise delimitation of these areas would be possible from aerial thermal images, terrestrial thermal monitoring or directly based on results of special-purpose meteorological measurements.

The above-characterized method of analyzing the spatial differentiation of temperature fields in urban and suburban landscapes is just one of several possible levels. Maps of surface temperature fields represent one of the usable outputs from a multilevel study of the urban and suburban climate of Olomouc, as a medium-sized city. The results achieved to date constitute a basis for subsequent studies of temperature regimes from special-purpose mobile or stationary meteorological measurements, possibly from terrestrial thermal monitoring.

Acknowledgement

The paper was prepared with the funding of Czech Grant Agency, project 205/09/1297 „Multilevel analysis of the urban and suburban climate taking medium-sized towns as an example".

References:

ALLEY, R. E., JENTOTF-NILSEN, M. (2001): Algorithm theoretical basis document for brightness temperature. Jet Propulsion Laboratory. Pasadena: [s.n.], 13 pp.

ASMAT, A. et al. (2003): Rule based classification for urban heat island mapping. In GIS tools for Application. [s.l.]:[s.n.], p. 61–71.

CAMPBELL, J. B. (2002): Introduction to remote sensing. 3rd ed. Taylor and Francis, London and New York. 621 pp.

DOBROVOLNÝ, P. (2011): Analýza teploty aktivních povrchů v oblasti Brna. In: Středová, H., Rožnovský, J., Litschmann, T. [eds]: Mikroklima a mezoklima krajinných struktur a antropogenních prostředí. Skalní mlýn, 2.–4.2. 2011, CD-ROM.

GANAS, A., LAGIOS, E. (2003): LANDSAT 7 night imaging of the Nissyros Volcano, Greece. International Journal of Remote Sensing, Vol. 24, p. 1579–1586.

GANGOPADHYAY, P. et al. (2005): ASTER-derived emissivity and coal-fire related surface temperature anomaly: a case study in Wuda, north China. International Journal of Remote Sensing [online]. 2005, Vol. 26, No. 24 [cit. 2008-01-20], p. 5555–5571. URL: Available at: <http://www.ingentaconnect.com/content/tandf/tres/2005/00000026/00000024/ art00014>.

GILLESPIE, A., et al. (1998): A temperature and emissivity separation algorithm for advanced spaceborne thermal emission and reflection radiometer (ASTER) images. Geoscience and Remote Sensing [online]. 1998, Vol. 36, No. 4 [cit. 2008-01-15], p. 1113–1126. Available at: WWW: <http://ieeexplore.ieee.org/Xplore/login.jsp?url=/iel4/36/15154/00700995.pdf?arnumber=700995>.

IEEE (2004): Aerospace Conference Digest. [online], 2004. 134 pp. Available at WWW: <http://www.aeroconf.org/2007_web/2004%20Digest%20rev101.pdf>.

JELÍNEK, K. (2008): Detekce tepelného ostrova města s využitím termálních snímků. [Diplomová práce] [Thesis]. Přírodovědecká fakulta MU, Brno, 87 pp.

LIANG, S. (2004): Quantitative remote sensing of land surfaces. John Willey & Sons. New Jersey:[s.n.], 534 pp.

MESEV, V. (1998): Remotely sensed cities. Taylor and Francis, London and New York, 2003, 378 pp.

NASA (2011): LANDSAT-5 web [online]. [cit. 2011-02-02]. Available at WWW: <http://landsat.usgs.gov/science_L5_Radiometric_LUT07.php >.

NASA (2011): ASTER Spectral Library [online]. 2011 [cit. 2011-02-02]. Available at: WWW: <http://speclib.jpl.nasa.gov/>.

NICHOL, J. E. (1998): Visualisation of urban surface temperatures derived from satellite images. International Journal of Remote Sensing, Vol. 19, p. 1639–1649.

OZAWA, A. et al. (2004): Aiborne hyperspectral and thermal information for assessing the heat island in urban areas of Japan. [cit. 2007-10-09]. Available at WWW: <http://www.isprs.org/istanbul2004/comm7/papers/9.pdf>.

QIN, Z., KARNIELI, A. (2001): A mono-window algorithm for retrieving land surface temperature from LANDSAT TM data and its application to the Israel-Egypt border region. International Journal of Remote Sensing [online], Vol. 22, No. 18 [cit. 2007-11-08], p. 3719–3746.

STUEVEN, B. (2004): A study of land cover and thermal changes at Kilauea volcano, Hawaii. 2004, [cit. 2011-25-01]. Available at: WWW: <http://www.uwlax.edu/urc/JUR-online/PDF/2004/stueven.pdf>.

VAN, T. (2007): Relationship between surface temperature and land cover types using thermal infrared remote sensing, in case of Ho Chi Minh city. [cit. 2007-11-20]. Available at: WWW: <www.fao.org/gtos/doc/ECVs/ T09/ECV-T9-landcover-ref08-Thi%20Van.doc>.

WENG, Q., LU, D. (2006): Spectral mixture analysis of ASTER images for examining the relationship between urban thermal features and biophysical descriptors in Indianapolis, Indiana, USA. Remote Sensing of Environment, No. 104, p. 157–167.

WENG, Q., LU, D., SCHUBRING, J. (2004): Estimation of land surface temperature–vegetation abundance relationship for urban heat island studies. Remote Sensing of Environment, No. 89, p. 467–483.

WENG, Q., YANG, S. (2006): Urban air pollution patterns, land use, and thermal landscape: an examination of the linkage using GIS. Environmental Monitoring and Assessment, No. 117, p. 463–489.

Satellite images:

LANDSAT: United States Geological Survey, http://glovis.usgs.gov

ASTER: ARCDATA PRAHA, s.r.o.

Authors' addresses:

Mgr. Jan GELETIČ, e-mail: *geletic.jan@gmail.com*
Assoc. Prof. RNDr. Miroslav VYSOUDIL, CSc., e-mail: *miroslav.vysoudil@upol.cz*
Palacky University Olomouc, Faculty of Science, Department of Geography
17. listopadu 12, 771 46 Olomouc, Czech Republic

Initial submission 13 March 2011**, final acceptance** 13 December 2011

Please cite this article as:

GELETIČ, J., VYSOUDIL, M. (2012): Analysis of surface temperatures in urban and suburban landscapes from satellite thermal images: a case study of Olomouc and its environs, Czech Republic. Moravian Geographical Reports, Vol. 20, No. 1, p. 2–15.

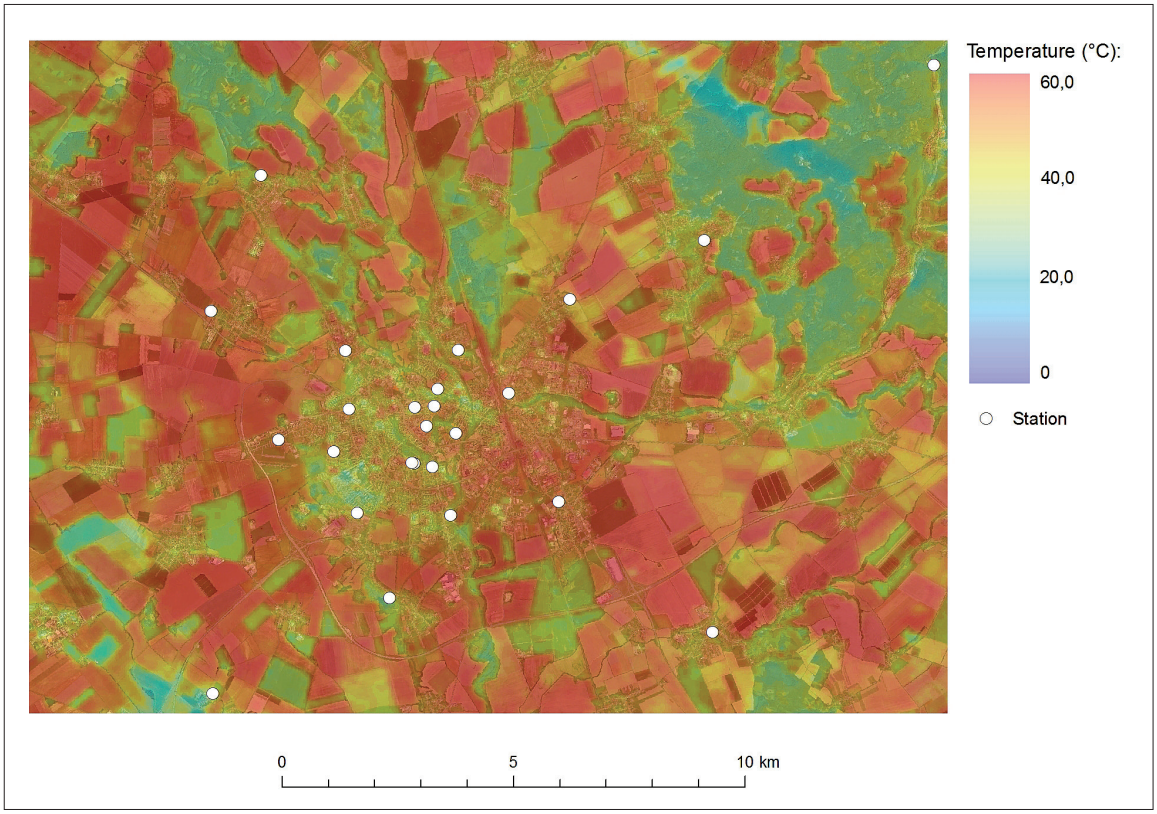

Fig. 7: Surface temperature field in Olomouc and its surroundings on 27th Sept. 2009 (source LANDSAT TM)

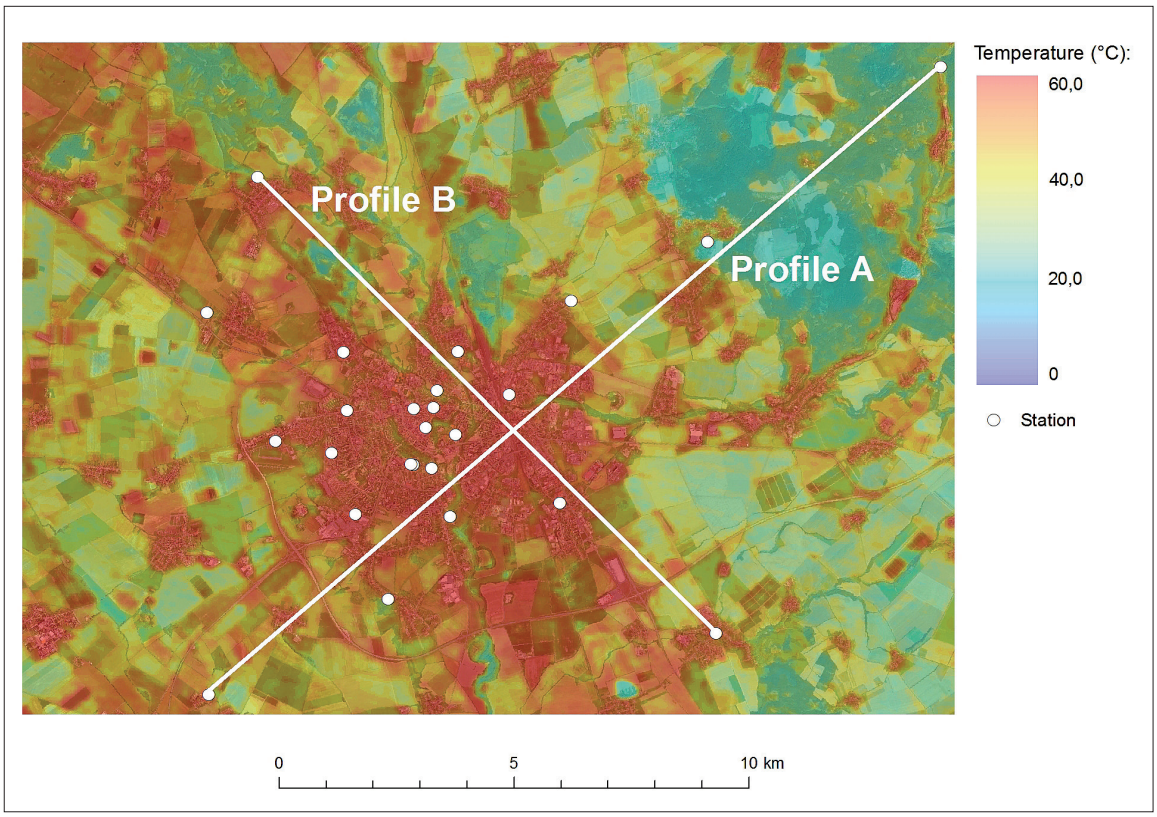

Fig. 8: Surface temperature field in Olomouc and its surroundings on 12th July 2010 and the line of surface temperature profiles a) BYST-DDHL, b) HORK-VTYN (source LANDSAT TM)

Illustration related to the paper by J. Geletič and M. Vysoudil